NASA Technical Memorandum 106007

Identification of Propulsion Systems

Walter Merrill and Ten-Huei Guo
Lewis Research Center
Cleveland, Ohio

and

Ahmet Duyar
Florida Atlantic University
Boca Raton, Florida

Prepared for a workshop
sponsored by the Ohio Aerospace Institute
Cleveland, Ohio, August 9, 1991

NASA

IDENTIFICATION OF PROPULSION SYSTEMS

Walter Merrill and Ten-Huei Guo
NASA Lewis Research Center
Cleveland, Ohio

and

Ahmet Duyar*
Florida Atlantic University
Boca Raton, Florida

Abstract

This paper presents a tutorial on the use of model identification techniques for the identification of propulsion system models. These models are important for control design, simulation, parameter estimation, and fault detection. Propulsion system identification is defined in the context of the classical description of identification as a four step process that is unique because of special considerations of data and error sources. Propulsion system models are described along with the dependence of system operation on the environment. Propulsion system simulation approaches are discussed as well as approaches to propulsion system identification with examples for both air breathing and rocket systems.

I. Introduction

The purpose of this paper is to present a tutorial on the use of model identification techniques for the identification of propulsion system models. The application of these techniques to identify models is important for several reasons. The simplified propulsion models obtained from identification are required for the design of propulsion control systems. Also, the identified models are often used for output estimation of important engine measurements for model based fault detection schemes. Third, identified models are often quite useful for real-time simulation of propulsion systems. Real-time simulation is required to evaluate hardware implementations of propulsion control systems. Finally, it is often important to apply identification techniques to obtain estimates of important engine parameters such as efficiencies or component performance parameters. These identified parameters can be used to improve control performance or to gain a better understanding of engine operation.

*Summer Faculty Fellow at NASA Lewis Research Center.

Identification is a four step process. First, system data is obtained from the system to be identified. Second, a model structure is identified. Third, model parameters which exist with the previously defined structure are identified. Finally, the model is verified by predicting known system behavior by comparing model predictions to system data not used in step three. This process applies to the identification of any system. What makes the propulsion application unique are the data and error sources associated with propulsion systems.

There are two data sources used to identify propulsion system models, an engine simulation and measurements taken from a real engine. The engine simulation is typically, a very detailed, highly nonlinear, digital simulation of equations which represent first principle models of the basic components of the engine. The sources of error for the simulation are limited to the precision of the computer(not a factor) and the modeling simplifications used in the development of the simulation. These simplifications include a finite number of lumped parameter, control volumes which are used to model what is truly a distributed process. The second data source was data obtained by measurement from a real engine. Sources of error in this case include errors in making the measurements, measurement noise, limited amounts of data(testing is expensive), and limited experiment design(data is often only available from experiments performed for another purpose). Also, the data obtained is almost always obtained from an engine with a control. Thus, the data obtained are closed-loop data which requires that the identification techniques applied must be able to eliminate the effect of the control. This process is never perfect and results in some additional error to the identified models.

The remainder of this paper will describe how propulsion systems are modeled in general. Then some specific model forms which admit the application of identification techniques will be discussed. Next, some successful applications of identification to propulsion systems will be described. Finally, the paper will close with some concluding remarks.

II. Propulsion System Models

Identification techniques have been applied to a wide variety of propulsion systems. To focus the discussion, a typical airbreathing engine shown in Figure 1 is used as an
example. Most propulsion systems have some of the elements embodied in this particular system, rotating turbomachinery, combustion processes, variable geometry, and multiple flow paths for the working fluid. For the engine of Figure 1 the major components: inlet, fan, etc. are labeled and the various numerical station designations are given.

As mentioned in the preceding section, a detailed, nonlinear simulation of the engine usually exists which predicts engine behavior. This is of the manufacturer's guaranteed specification of engine performance and is therefore, an accurate representation. Identification can be accomplished using data from this simulation. It will be helpful to understand how these simulations are created from physical models to further understand how identified models are generated.

Modeling the behavior of this engine will require a description of the environment in which the engine operates, first principles based equational descriptions of internal engine characteristics, pressures, temperatures, flow rates, and turbomachinery angular velocities (rotor speeds) and specific performance information associated with each component. Each of these three modeling elements is discussed below. A more complete description of engine modeling and simulation is given by Szuch[1].

Engine performance is dependent on its environment, specifically the temperature, pressure and velocity of the air entering the inlet. The ambient pressure of the air surrounding the engine is also important in finding the thrust developed by the engine. Since the engine exists in an airplane, the flight envelope of the plane is required. This envelope is specified in terms of the altitude and Mach number of the airplane. An example flight envelope is shown in Figure 2 along with the variation in temperature and pressure of the air for the envelope. By specifying a flight condition, i.e. altitude and Mach No., the corresponding engine inlet temperature and pressure can be specified.

Although engines are actually distributed processes, they are modeled using lumped parameter approximations to the equations of continuity of mass and energy. A schematic of the lumped control volumes (mixing volumes) chosen for the engine of Figure 1 is shown in Figure 3. Typical equations for the compressor mixing volume are

$$\frac{d\dot{w}}{dt} = \Sigma\, \dot{w}_{in} - \Sigma\, \dot{w}_{out} \tag{1}$$

$$\frac{d(\dot{w}u)}{dt} = \Sigma\, \dot{w}_{in} h_{in} - h\, \Sigma\, \dot{w}_{out} \tag{2}$$

where w dot is mass flow rate, u is internal energy, and h is enthalpy.

The most important variables in defining engine behavior are the rotor speeds. Typical dynamic behaviors for an engine can vary up to four times with changes in engine speed as shown in Figure 4.

To complete the model, these equations are combined with performance information for each of the component blocks of Figure 3. One example of component performance is the compressor performance map of Figure 5 which shows the compressor's pressure ratio versus its flow for different operating speeds.

It is clear from the preceding discussion that when information from each remaining volume and component is combined that the resultant model will be of substantial complexity. This complexity results in reasonable accuracy. However, this complexity makes this particular form of the model difficult to use for control design and analysis.

To be useful for control design and analysis the modeling approach should admit a compact and general equational representation. Additionally, the representation should contain enough mathematical structures to allow analysis. Three generalized equational representations have been used to model engines. These model forms are called nonlinear, bilinear, and pseudolinear.

The first form, called the nonlinear model, is given as

$$\dot{x} = f(x,u,\phi) \tag{3}$$

$$y = g(x,u,\phi) \tag{4}$$

where u represents independent variables, fuel flow and variable geometry settings, e.g.; x represents state variables, temperature, pressure and speeds, e.g.; y represents engine outputs, thrust, stall margin, etc.; and ϕ are the environmental variables, inlet pressure and temperature. The functions f and g are nonlinear vector functions that represent the full equation set typified by equations (1) and (2). The model of equations (3) and (4) lacks the structure necessary to allow control design.

A second model representation, called the bilinear model, is given as

$$\dot{x} = f(x) + g(x)\,u \tag{5}$$

This model retains much of the generality of the full nonlinear model but brings in additional structure by assuming that the independent (control) variables enter the process linearly. This model form has seen only limited use in the design and analysis of engine controls[2].

The third model type is the pseudolinear model given as

$$\dot{x} = A(y,\phi)x + B(y,\phi)u \tag{6}$$

$$y = C(y,\phi)x + D(y,\phi)u \tag{7}$$

Here A, B, C, and D are matrices which are determined at the operating conditions defined by y and ϕ. This representation has seen the most use due to the availability of linear design and analysis techniques. The next section will discuss how the system matrices of equations (6) and (7) could be determined.

III. Identified Models by Linearization

Due to the availability of an engine simulation model, often the simplest and most straightforward identification approach is to determine A, B, C, and D by linearization of the equations represented by (3) and (4). This can be accomplished computationally as follows.

1. Individually perturb state variables while holding constant the remaining state variables, u and ϕ. In equation form

$$A_{ij} = \frac{\Delta f_i}{\Delta x_j}(x_0,u_0,\phi_0) \tag{8}$$

$$C_{ij} = \frac{\Delta g_i}{\Delta x_j}(x_0,u_0,\phi_0) \tag{9}$$

2. Once A and C are known then u can be perturbed and a steady-state match enforced by calculating B and D to satisfy

$$\Delta x = (-A^{-1}B)\Delta u \tag{10}$$

$$\Delta y - C(-A^{-1}B)\Delta u = D\Delta u \tag{11}$$

An important consideration in this process is the size of the perturbations, Δx_j, used. They need to be large enough to significantly excite the equations for computational accuracy, yet, small enough to insure a region of linearity. Often multiple sizes are used and the results compared for consistency. Additionally, both positive and negative perturbations are used and the results averaged to remove nonlinear effects. The linearization approach is ubiquitous

throughout the propulsion controls design community.

IV. Closed Loop Identification

A typical engine control design cycle consists of developing a dynamic engine simulation from steady-state component performance data, designing a control based upon this simulation, and then testing and modifying the control in an engine test cell to meet performance requirements. This design cycle has been successful for state-of-the-art engines. However, for more advanced multivariable engines that exhibit strong variable interactions, this procedure will result in substantial trial and error modification of the control during the testing phase. One method to automate the design process and reduce control modification testing and development cost would be to identify accurate dynamic models directly from the closed loop test data. These identified models would then be used in conjunction with a synthesis procedure to systematically refine the control. Recent advances in closed loop identifiability (Ref. [3]) present a methodology for this direct identification of engine model dynamics from closed loop test data. This section describes the application of the Instrumental Variable/Approximate Maximum Likelihood (IV/AML) identification method (Ref. [4]) to simulated and actual closed loop F100 engine data (Ref. [5]). This study was undertaken to determine if useful dynamic engine models could be identified directly from closed loop engine test data.

The IV/AML method is applied to both simulated and actual closed loop test multiple input data. The IV/AML method is an output error identification method and was implemented in a combined iterative/recursive form. The test data studied in this report contains both measurement and process noise. The available closed loop engine test data records are each comprised of only 200 sample points. Since this is a relatively low number of sample points per operating record, the IV/AML method was selected for use because Monte Carlo tests have shown the method to exhibit reasonable convergence for a small number of samples (Ref. 4). The IV/AML approach is shown in Figure 6. A complete description of the Refined IV/AML method is given in Ref. 4.

A. Engine Model

The Pratt and Whitney F100 engine (Ref. 5) is a twin-spool low-bypass ratio after-burning turbofan. Four controlled variables are considered: main fuel flow (WF), exhaust nozzle area (AJ), compressor (fan) inlet variable guide vanes (CIVV), and the rear compressor variable guide vanes (RCVV). Three output variables are considered: engine fan speed (N1), engine compressor speed (N2), and augmenter entrance pressure (PT6). The engine

speeds are indicative of the dynamic response of the engine while PT6 is closely related to engine thrust. Globally the engine is modeled as

$$\begin{aligned} \dot{x} &= f(x,u,ALT,MN) \\ y &= g(x,u,ALT,MN) \end{aligned} \tag{12}$$

where x is the state vector, u is the control vector and y is the output vector. Engine operation is also dependent upon environmental variables altitude (ALT), and Mach number (MN). An engine operating point is defined as

$$\begin{aligned} f(x_{ss},u_{ss},ALT,MN) &= 0 \\ g(x_{ss},u_{ss},ALT,MN) &= y_s \end{aligned} \tag{13}$$

A third order behavioral model relating the engine outputs to the primary control variables WF and AJ was developed in Ref. [6] and is given as

$$\dot{X} = \begin{bmatrix} -1/\tau_1 & C_{HL} & C_{PL} \\ 0 & -1/\tau_2 & 0 \\ 0 & C_{LP} & -1/\tau_p \end{bmatrix} X + \begin{bmatrix} b_{FL} & 0 \\ b_{FH} & 0 \\ 0 & b_{AP} \end{bmatrix} u \tag{14}$$

This model represents linearized behavior in a small region about an operating point. Including CIVV and RCVV and writing in matrix form, the behavioral model becomes

$$\left(I + A_1 z^{-1}\right) x_k = B_1 z^{-1} u_k \tag{15}$$

B. Test Data Application

The F100 engine was tested in the Lewis Research Center altitude test facility to evaluate the F100 Multivariable Control (MVC) law (Refs. 4 and 5). During the same test period the "Bill of Material" (BOM) control was also evaluated as a baseline/backup control model. Thus, there are a variety of closed loop operating records obtained throughout the flight envelope with a number of different power input requests. The two multivariable data sets

used in this report were recorded at an ALT = 10,000 ft, MN = 0.9 condition as the power request was varied (step change) in a small (hopefully linear) range about intermediate engine power. One set corresponds to an MVC control test, the other to a BOM test. Data were sampled at T = 0.05 sec for a 10-second transient, which yields K = 200 points for each record in the data sets.

The BOM and MVC control structures, linearized at an operating point correspond to the structure of Figure 7. The reference point and control blocks are different however, for the two controls. The structure of Figure 7 is exactly the structure given in Ref. 2, 3. Since each control structure is fixed at a given operating point, strong system identifiability can be guaranteed if

$$RANK\left[\begin{array}{c|c} I & O \\ \hline F & L \end{array}\right] = n_u + n_y \qquad (16)$$

Or in other words, if

$$\det[L] \neq 0 \qquad (17)$$

The BOM and MVC reference point schedules do exhibit the characteristic of (17), therefore, a direct identification approach, such as IV/AML, can be successfully applied to the closed loop input/output data sets recorded in the Lewis test facility.

Sensor instrumentation dynamics for the input and output variables of interest are beyond the 20 radians/sec frequency range. Thus, sensor dynamics were initially ignored in the identification tests. Ambient noise statistics were obtained during steady-state engine operation. Standard deviations were calculated at the operating point for the sensed values. Signal to noise ratios (SNR's) were estimated based upon these ambient noise levels and the deviations of the various signals from their operating point values. In each case the SNR's show the level of noise to be small relative to the signal. Therefore, the identification results should be quite consistent and accurate.

Normalized WF from the BOM and MVC control tests is shown in Figure 8. This is typical of the engine inputs in these tests. Power spectrum analysis of these inputs shows a slightly higher frequency component in the MVC inputs. Although more total power is contained in the BOM inputs, most of the power is concentrated below 6 radians/sec.

The control inputs of Figure 8 were used in conjunction with a model

identified from simulation data (called model 1) to predict engine output. Comparing the predicted outputs of model 1 with the actual outputs, it was found that model 1 was unacceptable. No output was predicted well for either BOM or MVC data. Slight discrepancies between simulation and test data cannot account for large discrepancies between predicted and actual outputs.

To investigate this further the IV/AML method was applied directly to the MVC and BOM closed loop test data producing models 2 and 3, respectively. Model 1 was used as a starting point. Model 3 accurately reproduces the data, from which it was generated (BOM). Model 2 results are similar. In fact, Table I shows the residual error of all the outputs for models 1, 2 and 3 to be less than 1 percent. However, comparing parameters for models 1, 2 and 3 (see Table I) it can be seen that while A_1 remains essentially unchanged, elements of B_1 do change substantially. This implies a slightly overparameterized model structure which does account for the inability of model 1 to predict BOM and MVC engine data. This is true since an overparameterized model becomes specialized to the data from which it was determined. To determine which elements should be eliminated to remove the overparameterization, the following procedure was adopted[7].

First, a reasonably accurate initial model is assumed. In this case, models 2 and 3 were used. An initial covariance matrix

$$P_o = diag(p_{oi}) \tag{18}$$

is chosen where the p_{oi} are small to indicate small uncertainty in the model parameters. In the engine example

$$P_o = 10^{-7} I \tag{19}$$

was used. Next, the IV/AML method is applied for only a single iteration to data for which the model is overparameterized. The method now will be most sensitive to removing the uncertainty inherent in the extra parameters. Now, the diagonal elements of P_1 which correspond to accurate parameters will not change. However, the diagonal elements of P_1, p_{1l}, which correspond to extra parameters will change significantly. Thus, if

where ϵ is a positive threshold, the corresponding parameter a_l can be set to

$$|p_{1i} - p_{oi}| > \varepsilon p_{oi} \tag{20}$$

zero. The threshold was selected as

$$\varepsilon = 0.05 \tag{21}$$

for the engine data.

Three elements of P_1 satisfied (20) for both MVC and BOM data. The corresponding parameters were eliminated and this new structure applied to simulation data. The resultant IV/AML identified model is given as model 4 in Table I. A comparison of average fit error is quite comparable to model 1 with full B_1 and, in fact, shows improvement in the PT6 comparison.

Note that the eigenvalue associated with PT6 in model 4 represents a frequency of approximately 25 radians/sec which is slightly greater than the 20 radians/sec natural frequency of the PT6 sensor. Obviously, the PT6 sensor dynamics can no longer be completely ignored in the interpretation of the results. Additionally, since one mode models the sensor dynamics, a second mode may be required to model the PT6 engine mode. This was not pursued at this time however.

When used to predict BOM and MVC output data, model 4 was still unsatisfactory. Model 4 did predict N1(MVC), N2(MVC), and N2(BOM). However, N1(BOM) and especially PT6 for both data sets were not predicted well. The error in PT6 is somewhat expected from sensor and input bandwidth considerations. The N1(BOM) error was not expected however. Figure 9 compares predicted N1 data using model 4 to actual closed loop N1(BOM) data. Model 4 predicted N1 grossly follows the trend of the simulated data. Thus, it appears that the dynamic portion of model 4 is correct. However, there must then be large discrepancies in some of the model 4 gain terms. These discrepancies are somewhat perplexing since model 4 predicted N1(MVC) but not N1(BOM).

Recall, however, that the BOM inputs are larger in magnitude than the MVC inputs, and that model 4 represents linearized dynamics. Thus, some nonlinear effects may be inherent in the BOM data. This explanation is not entirely satisfactory since N2(BOM) and N2(MVC) were both predicted. Further work to resolve this problem is required. The IV/AML identification method was again utilized to further refine the model parameters for the structure of model 4 using the two sets of experimental closed loop data. The

purpose of this final iteration is to identify a single model that can accurately predict both sets of engine test data and, hopefully, simulation data as well.

Again model 4 was used as an initial condition in the IV/AML method applied to the BOM and MVC data. Models 5 and 6 of Table I resulted. Both models 5 and 6 fit their respective data sets quite well. Similar comparisons to MVC data were obtained using model 6. More importantly, when the BOM model 5 is used to predict the MVC data, the comparison given in Figure 10 is quite reasonable. Thus, model 5 (or equivalently model 6) represents a model which predicts a class of inputs and can be used with confidence in a control design procedure.

V. Identification by Canonical Forms

In this section the development of an accurate representation of the dynamic behavior of the Space Shuttle Main Engine (SSME) is presented. The model is obtained by identification of linearized dynamic models of the SSME from a nonlinear dynamic simulation. The identified linearized models are valid in limited response regions about several operating points corresponding to the different power levels. The models are useful for real time estimation and fault detection as well as open loop engine dynamic studies and closed loop control analysis using a user generated control law.

A multivariable identification and a minimal realization technique[8,9] is used to identify these models in α-canonical form. Also, the development includes an technique for piecewise linear systems with static nonlinear gains, which is used in modeling the dynamics of the SSME.

Initially a brief description of the SSME is given. This is followed by a description of the identification scheme and the model used. Finally, results obtained from the identified models are compared with the results obtained from the nonlinear simulation for the same input.

A. The Space Shuttle Main Engine

Different aspects of the SSME as well as its principles of operation are described in the literature[10]. For the sake of completeness a brief description of the main engine is also given below.

The space shuttle orbiter main propulsion system is composed of three main engines. The engines use liquid oxygen and liquid hydrogen propellants carried in an external tank attached to the orbiter. To understand the overall flow of fuel and oxidizer to produce the thrust, a schematic diagram of the

propellant flows and the control valves is shown in Figure 11.

The two high pressure turbines are driven by a fuel turbine preburner and an oxidizer turbine preburner, each of which produces hot gas. The low pressure turbines are driven by the high pressure pump flows. The fuel from the high pressure fuel pump (HPFP) goes through the main fuel valve (MFV). After the MFV, the flow divides into fixed nozzle cooling flow, main chamber cooling flow, and coolant control valve (CCV) flow. Heat is absorbed from the combustion chamber and nozzle. The fixed nozzle cooling and the coolant control valve flows then recombine and travel to the preburners where combustion and pressure are controlled by the fuel preburner oxidizer valve (FPOV) and the oxidizer preburner oxidizer valve (OPOV). Main chamber coolant flow is used to drive the low pressure fuel turbopump.

The existing control system of the SSME uses five valves; FPOV, OPOV, MFV, MOV, and CCV. They control the mixture ratio and the main chamber pressure which is correlated with the thrust. Open and closed loop control of these valves are used to accomplish the SSME mission. For the purpose of model identification of the open loop system, the rotary motion of the five valves (β_{OPOV}, β_{FPOV}, β_{CCV}, β_{MOV}, β_{MFV}) is used as input. The outputs are the chamber pressure, P_C, and the mixture ratio, MR.

In a previous study[10] it was shown that β_{CCV}, β_{MOV}, and β_{MFV} valve rotary motions are essentially decoupled from the outputs during the main stage of operation. In this study, only the valve rotary motions, β_{FPOV} and β_{OPOV}, are used as the inputs of the open loop system.

B. System Identification

The steps used in identification of the SSME consist of: (1) selection of a driving signal with persistent excitations, (2) selection of a model, (3) parameter and structure estimation, and (4) model verification. These steps are followed for the identification of the SSME and are outlined below.

Selection of a Driving Signal

Selection of an appropriate input signal is an important step in identification problems. A basic criterion for this selection is that the input/output data should be informative enough to discriminate between different models among the class of models being considered. Without this discrimination there is no guarantee that the obtained parameters are the true parameters of the system. This criterion can be expressed mathematically in terms of the covariance matrices of the input signals and the order of the system being identified[11]. Uncorrelated pseudo random binary sequences which are used

in this study are examples of such input signals which can be used for designing an informative experiment.

Pseudo random binary sequences (PRBS) are selected as the input perturbation signals to excite the system because of their convenience and suitability for similar applications[12]. Two uncorrelated sequences, which satisfy the requirement of persistent excitation, are used for OPOV and FPOV inputs. The sequences have a clock time of 0.04 sec and a length of 127. This corresponds to a maximum frequency on 78.5 rad/sec (12.5 Hz), a minimum frequency of 1.24 rad/sec (0.2 Hz) and a signal duration of 5.08 sec.

Selection of a Mathematical Model

It is assumed that the nonlinear dynamics of the SSME can be described by discrete, linearized equations at a nominal operating condition:

$$\delta x(k + 1) = A\, \delta x(k) + B\, \delta u(k) \tag{22}$$

$$\delta y(k) = C\, \delta x(k) \tag{23}$$

where δx, δu, and δy are the deviations of the state, the input, and the output vectors about the nominal operating condition. It is assumed that the system described by equations (22) and (23) is stable and observable and the C matrix has full row rank.

Parameterization of A, B, and C is an important issue for identification of multi-input multi-output (MIMO) systems since they admit more than one parametrization depending on their observability indices. Thus, in order to obtain a minimal parametrization for MIMO systems, the structure of the system i.e., the observability indices related to each output must be determined. Recently[8], the notion of output injection was employed to obtain a new canonical form for a special class of observable systems. Through this canonical form, a structure and parameter identification algorithm was developed for a restricted class of systems. This technique was extended to the class of all minimal systems and the output injection was constrained by an extra condition to guarantee the uniqueness of the parametrization[9].

When the system of (22) and (23) is realized in α-canonical form, i.e., the following relations hold:

$$C = \left[0 : H^{-1}\right] \tag{24}$$

$$A = A_o + KHC, \text{ with } A_o^{\mu} = 0 \tag{25}$$

$$(HC)_{r_i} A_o^{\mu_i} = 0 \tag{26}$$

$$(HC)_{r_i} A_o^{k} K_{c_j} = 0, \quad \text{for} \quad \mu_i > \mu_j \quad \text{and} \quad k < \mu_i - \mu_j \tag{27}$$

Here the subscripts r_i and c_j denote the i'th row and j'th column respectively. Superscripts indicate exponentiation. The structure matrix A_o is lower left triangular and consists of zeros and ones only and is determined by the observability indices, μ_i where i associates μ_i with the i'th output and $\mu = \max\{\mu_i\}$. The matrix K is a deadbeat observer gain.

In the following section a parameter and structure identification scheme for the above system is given. It is assumed that H matrix is equal to the identity matrix, I. The generalization of this identification scheme to the case with $H \neq I$ is also possible[9].

Identification of Linear Models

The process of α-canonical identification includes five steps. First, the observability indices, μ_i, are determined. Second, the matrix A_0 is constructed. Third, the measured outputs are transformed by the H matrix. Fourth, the deadbeat observer gain, K, is estimated. Finally, the matrix B is estimated. This then yields the model for the process as

$$\delta y(k) = \sum_{i=1}^{\mu} CA_o^{i-1}[K \; B] \begin{bmatrix} \delta y(k - i) \\ \delta u(k - i) \end{bmatrix}, \quad \text{for} \quad k \geq \mu \tag{28}$$

Identification of Piecewise Linear Models

The five step procedure is used to identify the open loop system dynamics of the SSME at different power levels. The responses of the identi-

fied open loop system are compared with the responses obtained from the nonlinear simulation. In general, it is observed that the gains for positive and negative perturbation signals are significantly different. In order to compensate for this phenomenon, a system gain with different values for positive and negative perturbations is added to the linearized model.

With this modification the system equations become

$$\delta x(k+1) = A\,\delta x(k) + B\,\delta u^{*}(k) \tag{29}$$

$$\delta y(k) = C\,\delta x(k) \tag{30}$$

where $\delta u^{*}(k)$ is defined component-wise as

$$\delta u_i^{*} = \begin{cases} \lambda_i \delta u_i(k) \text{ , for } \delta u_i(k) \geq 0 \\ (2 - \lambda_i)\delta u_i(k) \text{ , for } \delta u_i(k) \leq 0 \end{cases} \tag{31}$$

Results

Using the above procedure and the identification algorithm summarized in this section, the parameters of the piecewise linear model described by equations (34) to (36) are identified at 70, 80, 90, 100, and 110 percent power levels. As mentioned earlier, the input vector, δu, represents the deviations of the valve rotary motion from the nominal values defined as:

$$\delta u = \left[\delta\beta_{OPOV}\ \delta\beta_{FPOV}\right]^{T} \tag{32}$$

The output vector δy represents the deviations of the chamber inlet pressure and the mixture ratio from their nominal values and defined as:

$$\delta y = [\delta P_c\ \delta MR]^{T} \tag{33}$$

The A,B,C matrices and the nonlinear gains λ_1 and λ_2 of the identified piecewise linear model are given in Table II.

The validity of the estimated parameters of the system is checked by comparing the responses obtained from the identified system with the response of the nonlinear simulation. Both a state variable filter and the model

of the identified system are used for comparison purposes. The state variable filter utilizes the measurements of both the output δy, and the input, δu, to estimate the next value of the output, $\delta y_f(k)$, defined as

$$\delta y_f = \sum_{i=1}^{\mu} CA_o^{i-1} [K \; B] \begin{bmatrix} \delta y(k - i) \\ \delta u^*(k - i) \end{bmatrix} \tag{34}$$

The model of the identified system utilizes only the measurement of the input data, δu, to predict the output, δy_m, and the state, $\delta \hat{x}$, as

$$\delta \hat{x}(k + 1) = A\delta \hat{x}(k) + B\delta u^*(k) \tag{35}$$

$$\delta y_m(k) = C\delta \hat{x}(k) \tag{36}$$

Two different test input signals are used for comparison purposes. The first test input signal consists of two full length PRBS (different PRBS than the ones used for identification purposes) which cover the same frequency range as those used for identification. The second test signal consists of step and ramp inputs and covers a lower frequency range than the range of validity of the identified system.

The comparison of the responses of both the identified model and the filter to the responses obtained from the nonlinear simulation of the SSME for low frequency test signals also indicate good agreement.

VI. Fault Detection by Identification

A distributed model based fault detection and diagnosis system based on an on-line recursive version of the α-canonical identification method presented above is described in this section. The process is assumed to be a piecewise linear time invariant system described as:

$$\begin{aligned} X(t+\Delta T) &= A(X_o)X(t) + B(X_o)U(t) \\ Y(t+\Delta T) &= C(X_o)X(t+\Delta T) \end{aligned} \tag{37}$$

Where ΔT is the data sampling time and X_o represents the state of the selected operating point.

The piecewise linear model with identified parameters is used as the *a priori* knowledge of the diagnostic scheme. The basic architecture of this diagnostic system[13] is described in Figure 12. It assumes that there are

three failure mode classes to be identified: System Degradation, Actuator Failure and Sensor Failure. It also assumes that within the neighborhood of the operating condition, the major impact of a System Degradation is on matrix *A*, actuator failures will be reflected by the changes of matrix *B* and Sensor Failures can be related to *C*. In Figure 12, each condition monitor module is constructed to detect a specific class of failure modes. For example, an actuator failure detector is using the known information of $A(X_o)$ and $C(X_o)$ to estimate the actuator matrix *B* and its structure. The estimated parameters are then converted into a set of simple indicators for specific failure modes within the class of actuator failure modes. The on-line estimated model error is used as an indicator of the confidence level of the hypothesis (i.e. the higher the model error the lower the confidence of the hypothesis). The SSME (Space Shuttle Main Engine) actuator failure modes are used as the example to demonstrate the feasibility of the approach. The results of the study show that the simulated actuator failures can be correctly identified within a reasonable time period.

Furthermore, if the system is to be operated over a wide range and a linear model can not accurately represent the system characteristics then a series of parameter identifications will be needed to cover the possible range of operation conditions. A piecewise linear model which links all the operation conditions can be described by:

$$\begin{aligned} x(n+1) &= A(y_s)\, x(n) + B(y_s)\, u(n) \\ y(n) &= C(y_s)\, x(n) \end{aligned} \qquad (38)$$

where y_s is the scheduling variable and is a subset of the output measurement y.

A. Modeling the Process Faults

In general, there are three classes of fault modes covered by the system performance model of equation (1), namely actuator faults, sensor faults and system performance degradation. In this study, actuator faults are modelled by the changes of actuation gain matrix B. Sensor faults are modelled by the changes of observation matrix C. System performance degradations (dynamic changes) are modelled by the system characteristic matrix A. Under these assumptions, these fault modes can be isolated and diagnosed by analyzing the observed behavior through hypothesis testing which will be described latter.

For a complete model that describes all three possible classes of faults the system equation will be:

$$x(n+1) = (A + \Delta A)\, x(n) + BF_a\, u_c(n) + Bf_{ao}$$
$$y_{sf}(n) = F_s C\, x(n) + f_{so} \qquad (39)$$

We now define F_s, f_{so}, F_a, f_{ao} and ΔA as fault parameters. The s subscript indicates sensor faults, the a subscript indicates actuator faults, F is a multiplicative error, f is a bias error, and the ΔA is the fault parameter that indicates system degradation. The following section describes the strategy of detecting the fault and estimating the fault parameters using a distributed on-line parameter identification scheme.

B. Fault Detection and Diagnosis

In the fault-detection and diagnosis for the system modelled by (39), one approach is to have an on-line estimation algorithm for all fault parameters in the equation. The estimated fault parameters can be compared to the predetermined signature of the fault modes of different classes. With this approach it is difficult to estimate many fault parameters at the same time. Also, the signatures of the fault parameters can be ambiguous if they were estimated by a single module. Thus, instead of direct estimation of parameter matrices A, B, C, and their related fault parameters, a two-step approach is proposed. In the first step a group of "Hypothesis Testing Modules" (HTM) are processed in parallel to test each class of faults. Each module is solely designed to process the input/output data under a specified hypothesis and generate the fault signature data for diagnostics purposes. The second step is the fault diagnosis module which checks all the information obtained from the HTM level, isolates the fault, and determines its magnitude. Figure 13 shows the structure of the fault detection and diagnostic system.

C. Application to the SSME

The signature of a fault mode can usually be obtained through the analysis of physical properties or empirical data. In the Space Shuttle Main Engine the commonly observed actuator faults can be classified into four types: valve ball seal leakage or crack, valve line blockage, stuck valve and loss of rotational variable displacement transformer (RVDT) signals[14]. A ball seal leakage may cause increased flow rate through the valve for the same actuator input, causing the fault vector parameter f_{ao} to have a nonzero component associated with the faulty valve. The value of this nonzero element yields the amount of leakage. A shaft seal leakage may cause a diaphragm rupture and consequently a stuck valve. This would cause those elements of F_a and f_{ao} associated with the faulty valve to change from a value of one to a value of zero and from a value of zero to a nonzero value respec-

tively. A broken wire in the RVDT system may lead to a signal error, causing the valve to continuously increase its opening until it is fully open. Table III describes part of these fault signatures, i.e., it gives the values of the fault parameters corresponding to each signature as well as the values for some combinations of these faults.

A nonlinear simulation is used to simulate the SSME dynamic responses for nominal operation and fault conditions. The inputs of the simulation are the positions of the oxidizer preburner oxidizer valve (OPOV), and fuel preburner oxidizer valve (FPOV). The measured simulation outputs are the chamber inlet pressure (Pc) , mixture ratio (MR), high pressure fuel turbine speed (SF2), and high pressure oxidizer turbine speed (SO2). The operating condition selected for study is at 100% rated power level with nominal mixture ration of 6.026. A closed loop control (PI controller) in the simulation is also active to simulate the actual operation. The sampling time of the system identification is 0.04 second. Pseudo random binary sequences (PRBS) with a magnitude of 1% of the control command are superimposed on the command signal. A recursive parameter identification scheme is used to identify the fault parameters for the case where the OPOV fails.

Figure 14 shows a case in which the OPOV stuck at time of 1.0 second. In this case the valve stopped responding to the input command. The expected parameter values for this type of fault are $F_a11 = 0$, $F_a22 = 1$, $f_{ao}1 = C_{bias}$ (the magnitude of bias depends on the valve stuck position and the desired position of the operating condition) and $f_{ao}2 = 0$. Terminology used to label fault parameters are $F_a(1,1) = F_a11$, $f_{ao}(1) = f_{ao}1$, etc. The simulation shows that the diagnostic system is not only able to identify the correct actuator fault type after the initial transient but also able to estimate the magnitude of the bias due to the fault which can be very important in designing the control accommodation for the fault. Figure 15 shows the on-line calculated residual defined by equation (10) under the hypothesis of an actuator fault. Values of the residual vector return to approximately zero after the initial transient. Figure 16 shows the residual values calculated by the module which hypothesizes system degradation faults. In this figure, the residual vector elements are at least ten times higher than those in Figure 15. Similarly large residual values were computed by the third module. It can be seen that these values can be used to test the validity of the hypothesis modules.

A second example is for a bias in the Chamber Pressure (Pc) Sensor. Figure 17 shows the results obtained for the case of a faulty sensor with a bias of 1% on sensor one (chamber pressure). As expected, the results are that the estimated fault parameters $F_s \approx I$ and the bias terms $f_{so} \approx 0$ except $f_{so}1$ which is the indicator of Pc measurement bias.

As illustrated in these simulation results, both the fault-detection and the estimation of the extent of faults can be determined by using the proposed approach. These simulations indicate that a duration of two seconds is sufficient for the fault detection and diagnosis.

VII. Concluding Remarks

In this paper the authors have discussed the importance of propulsion system identification as a tool to develop propulsion models for control design, simulation, parameter estimation, and fault detection. The notion of propulsion system identification was defined in the context of the classical description of identification as a four step process. Propulsion system identification was shown to be unique because of the special considerations of data and error sources. Propulsion system models were described. Three model formulations were described, nonlinear, bilinear, and pseudo-linear. The dependence of system operation on the environment was described. Propulsion system simulation approaches were discussed because of the important role that simulation plays in the controls design cycle. Finally, some approaches to propulsion system identification were explained with examples for both air breathing and rocket systems. Three approaches were given, linearization of simulation equations, closed-loop identification from test data, and identification via canonical forms. Results of these approaches were presented. Also presented was the use of an identification approach to detect faults in a propulsion system.

References

1. Szuch, J. R., "Models for Jet Engine Systems-Pt. 1, Techniques for Jet Engine Systems Modeling," *Control and Dynamic Systems-Advances in Theory and Applications, Vol. 14, edited by C. T. Leondes, Academic Press, New York, 978, pp.213-257.*

2. Phillips, S., and Mattern, D.: "Feedback Linearization for Control of Air Breathing Engines." AIAA-91-2000, presented at the 27th Joint Propulsion Conference, 1991.

3. Soderstrom, T.;Ljung, L.; and Gustavsson, I.: "Identifiability Conditions for Linear Multivariable Systems Operating Under Feedback." IEEE Trans. of Autom. Control, Vol. AC-21, No. 6, Dec. 1976, pp. 837-840.

4. Jakeman, A., and Young, P.: "Refined Instrumental Variable Methods of Recursive Time-Series Analysis - Part II, Multivariable Systems." Int. J. Control, Vol. 29, No. 4, 1979, pp. 624-644.

5. Lehtinen, F. B.; Costakis, W. G.; Soeder, J. F.; and Seldner, K.: "F100 Multivariable Control Synthesis Program-Results of Engine Altitude Tests." NASA TM S-83367, 1983.

6. DeHoff, R.; Hall, W. E., Jr.; Adams, R. J.; and Gupta, N. K.: "F100 Multivariable Control Synthesis Program. Vols. I and II," AFAPL-TR-77-35, June 1977. (AD-A052420 and AD-A052346.)

7. Merrill, Walter C.: "Identification of Multivariable High Performance Turbofan Engine Dynamics from Closed Loop Test Data." Sixth IFAC Symposium on Identification and System Parameter Estimation, Washington, DC, June 7-11, 1982. NASA TM-82785, December 1981.

8. Eldem, V. and Yildizbayrak, N.: "Parameter and Structure Identification of Linear Multivariable Systems," Automatica, 24, 365-373, 1988.

9. Eldem, V. and Duyar, A.: "Identification of Discrete Time Multivariable Systems: A Parameterization Via α-Canonical Form," submitted to Automatica for publication, 1989.

10. Duyar, A, Guo, T. and Merrill, W.: "Space Shuttle Main Engine Model Identification," IEEE Control Systems Magazine, Vol. 10, No. 4, pp. 59-65, 1990.

11. Ljung, L.: *System Identification: Theory for the User*, Prentice Hall, 1987.

12. Cottington, R.V. and Pease, C.B.: "Dynamic Response Testing of Gas Turbines," Journal of Engineering for Power, Trans. of the ASME, 1-6, 1978.

13. A. Duyar, V. Eldem, W. C. Merrill and T.-H. Guo: "A Simplified Dynamic Model of Space Shuttle Main Engine," Submitted to ASME Journal of Dynamic Systems Measurement and Control, June 1990.

14. Tischer, A.E . and Glover, R. C., "Studies and Analyses of the Space Shuttle Main Engine," Prepared for NASA George C. Marshall Space Flight Center, Contract No. NAS8-3737, December 1987.

Table I Identified model Parameter values

Model	Model data source	Number of data points	A_1	B_1	C_1	$Qx10^5$	Percent error
1	Simulation	400	-0.840 0 0 0 -.858 0 .382 -.120 -.396	0.0405 0.0395 0.0005 -0.0032 .0235 .0102 .0006 .0029 .2133 -.3362 -.0026 -.0318	-0.970 0 0 0 -.978 0 .092 0 -.977	0.225 0.056 -0.314 .056 .040 .171 -.314 .171 4.486	0.421 .489 .581
2	MVC test	200	-0.865 0 0 0 -.801 0 .368 -.124 -.344	0.0405 0.0442 0.0029 -0.0002 .0318 .0088 -.0023 -.0002 .1937 -.3284 -.0672 -.0022	-0.951 0 0 0 -.960 0 .108 0 -.971	0.189 0.046 0.021 .046 .017 .064 .021 .064 2.692	0.431 .264 .894
3	BOM test	200	-0.850 0 0 0 -.836 0 .379 -.119 -.346	0.380 0.0405 0.0017 -0.0003 .0324 .0112 .0012 -.0004 .2092 -.3343 -.0221 .0155	-0.982 0 0 0 -.971 0 .086 0 -.974	0.189 0.046 0.021 .046 .017 .064 .021 .064 2.692	0.117 .185 .524
4	Simulation	400	-0.700 0 0 0 -.859 0 .264 -.189 -.293	0.0631 0.0769 -0.0032 0 .0245 .0110 0 0 .1862 -.5070 -.0338 -.0415	-0.974 0 0 0 -.988 0 .060 0 -.960	Same as above	0.550 .469 .375
5	BOM test	200	-0.670 0 0 0 -.818 0 .266 -.189 -.283	0.0378 0.0465 -0.0095 0 .0290 .0066 0 0 .1701 -.4981 -.0474 .0116	-0.982 0 0 0 -.973 0 .048 0 -.965	Same as above	0.115 .205 .528
6	MVC test	200	-0.728 0 0 0 -.808 0 .255 -.194 -.291	0.0508 0.0805 -0.0028 0 .3030 .0193 0 0 .1801 .4989 -.0842 -.0034	-0.951 0 0 0 -.964 0 .059 0 -.958	Same as above	0.425 .275 .754

Table II Identified values of system matrices

Power level, percent	A				B		C				λ_1	λ_2
70	0	0	-0.2553	0.0416	0.3923	0.0958						
	0	0	0.5044	-0.1108	1.0558	-0.2652	0	0	1	0	0.8957	0.8403
	1	0	1.0218	-0.113	0.2584	0.0788	0	0	0	1		
	0	1	-0.7902	0.5812	0.5902	-0.2697						
80	0	0	-0.1576	0.0257	0.4068	0.1564						
	0	0	0.2587	-0.0545	0.9631	-0.674	0	0	1	0	1.1211	0.9279
	1	0	0.8759	-0.0666	0.2574	0.0384	0	0	0	1		
	0	1	-0.5157	0.4766	0.6046	-0.2307						
90	0	0	-0.1206	0.0155	0.4223	0.1546						
	0	0	0.1434	-0.0275	0.9217	-0.7302	0	0	1	0	0.9386	0.7699
	1	0	0.8117	-0.0478	0.2518	0.021	0	0	0	1		
	0	1	-0.4183	0.4226	0.6288	-0.1779						
100	0	0	-0.1279	0.0212	0.3534	0.0475						
	0	0	0.1994	-0.0508	0.6831	-0.6446	0	0	1	0	0.8594	0.9047
	1	0	0.7816	-0.0565	0.2007	-0.0181	0	0	0	1		
	0	1	-0.5253	0.475	0.5043	-0.1387						
110	0	0	-0.084	0.0026	0.2416	0.0786						
	0	0	0.1082	-0.0123	0.5112	-0.575	0	0	1	0	0.9704	1.1231
	1	0	0.728	0.0181	0.1456	-0.0243	0	0	0	1		
	0	1	-0.4164	0.333	0.3593	-0.078						

Table III SSME Actuator Fault Signatures

ACTUATION FAILURE MODE	FAULT PARAMETERS			
	Fa11*	Fa22	fao1**	fao2
NORMAL	1	1	0	0
OPOV VALVE BALL SEAL LEAKAGE	1	1	C_1^+	0
FPOV VALVE BALL SEAL LEAKAGE	1	1	0	C_2
FPOV and OPOV VALVE BALL SEAL LEAKAGE	1	1	C_1	C_2
OPOV BLOCKAGE	1	1	$-C_1$	0
FPOV BLOCKAGE	1	1	0	$-C_2$
OPOV VALVE BALL SEAL LEAKAGE FPOV BLOCKAGE	1	1	$-C_1$	$-C_2$
OPOV VALVE STUCK	0	1	C_1	0
FPOV VALVE STUCK	1	0	0	C_2
OPOV & FPOV VALVE STUCK	0	0	C_1	C_2
OPOV RVDT FAILURE	0	1	C_1	0
FPOV RVDT FAILURE	1	0	0	C_2
OPOV and FPOV RVDT FAILURE	0	0	C_1	C_2

* Fa11 indicates the 1,1 element of the Fa matrix

** fao1 indicates the 1st element of the fao vector

+ C_1 & C_2 represent the bias terms

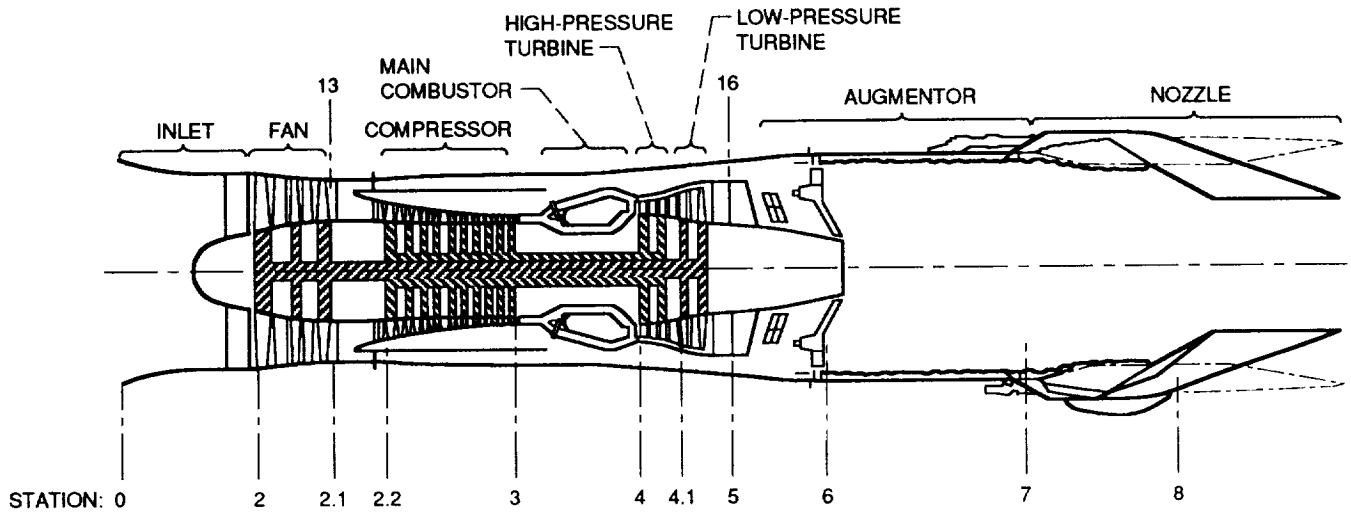

Figure 1.—A typical airbreathing engine schematic.

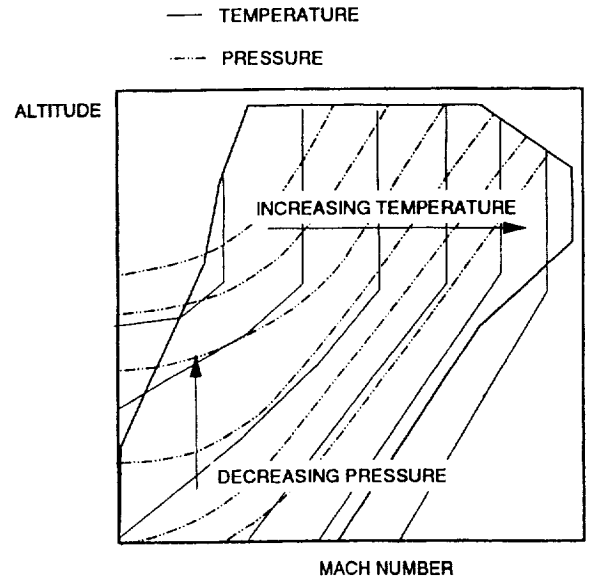

Figure 2.—Example flight envelope.

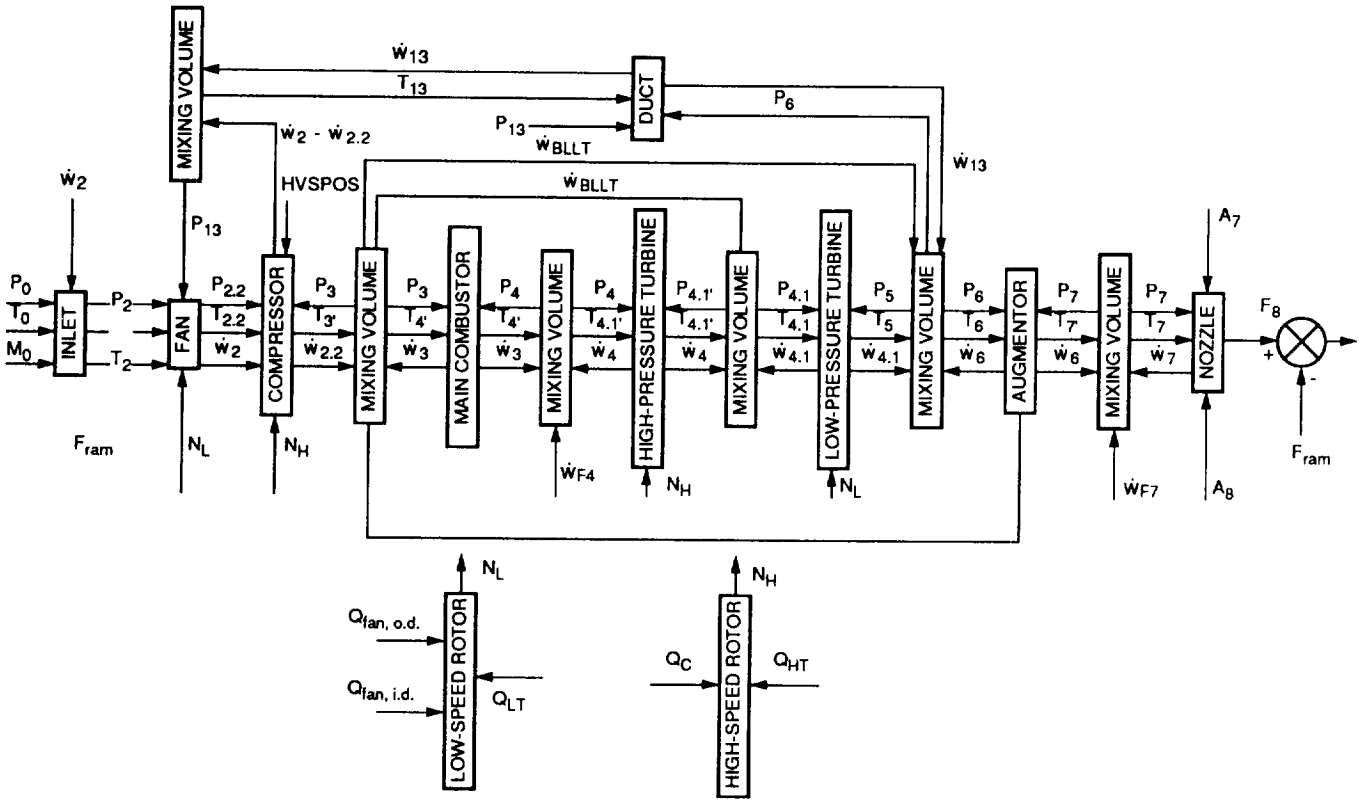

Figure 3.—Engine simulation schematic.

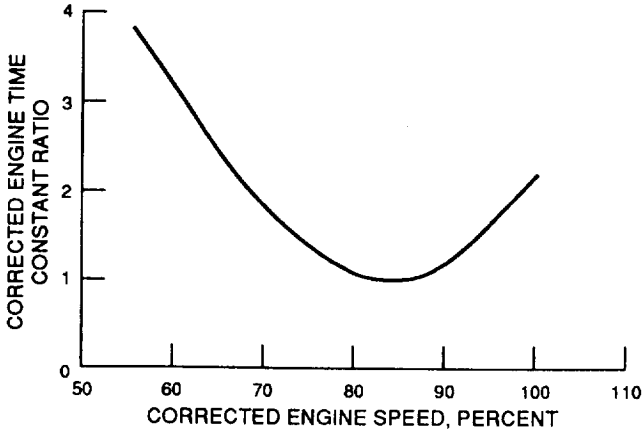

Figure 4.—Typical engine dynamic behavior.

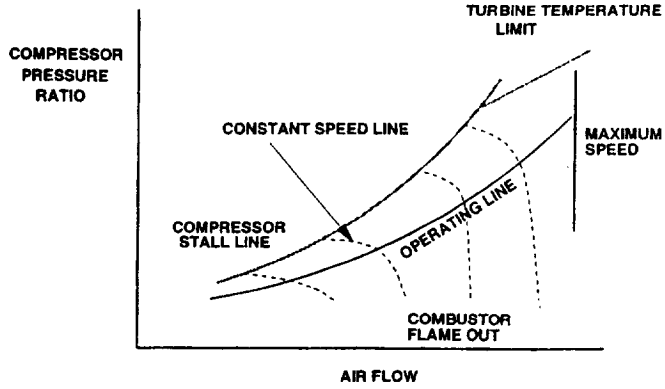

Figure 5.—Compressor performance map.

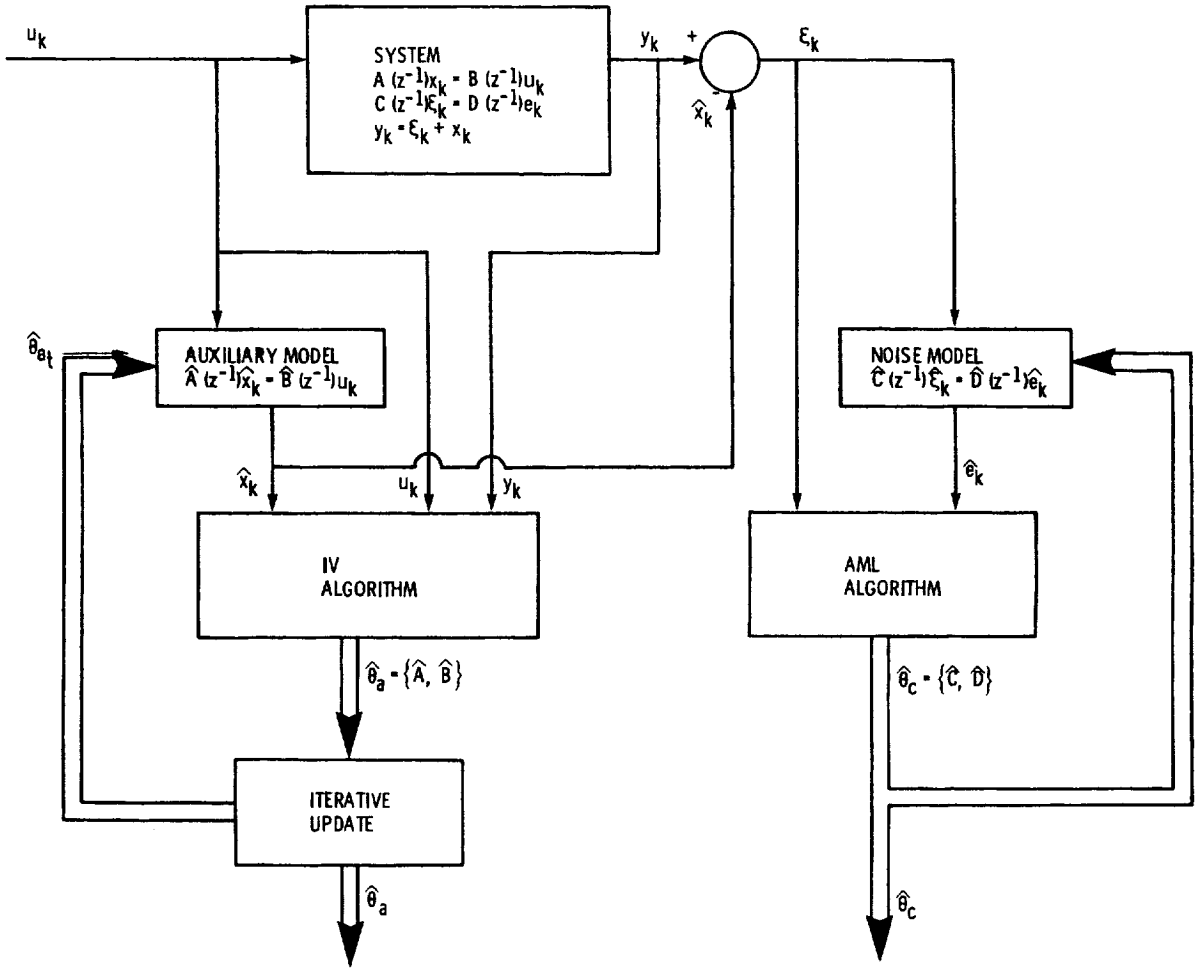

Figure 6.—The instrumental variable/approximate maximum likelihood approach.

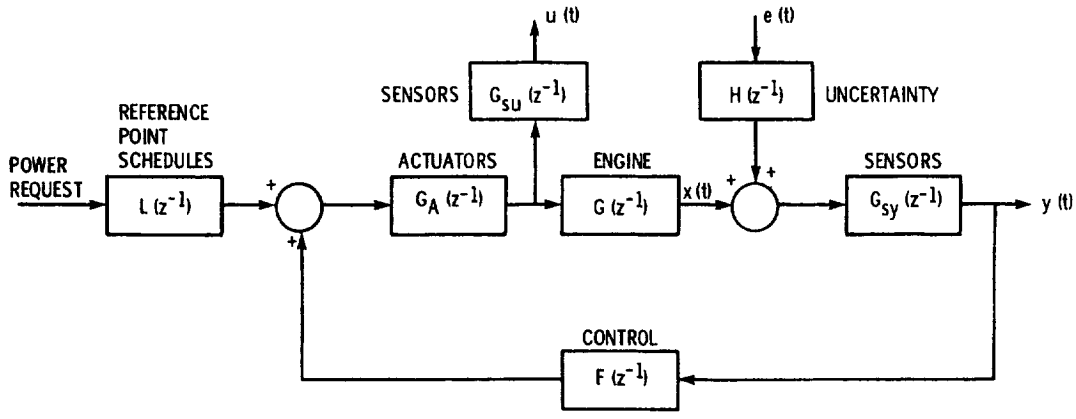

Figure 7.—Feedback control structure.

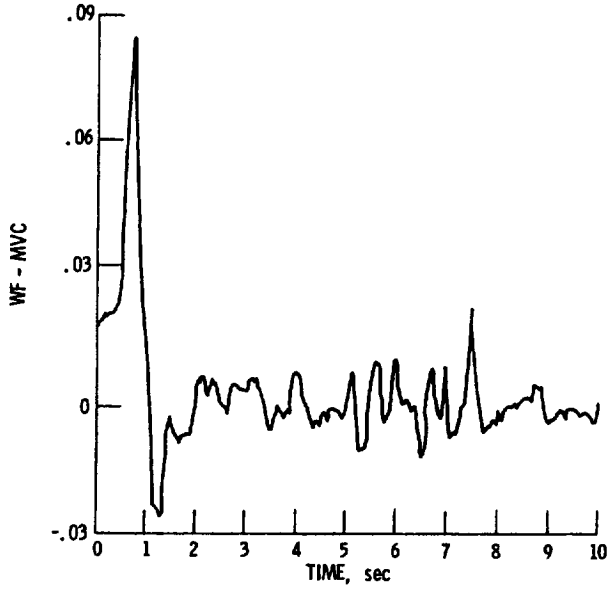

Figure 8.—Normalized control inputs.

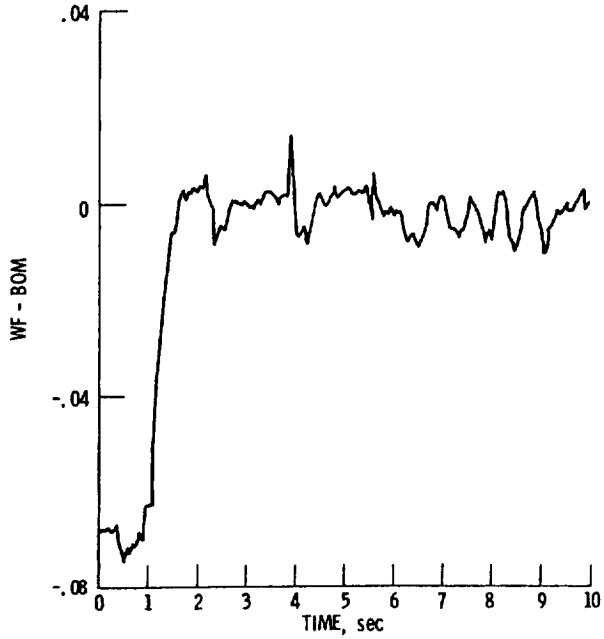

Figure 8.—Concluded.

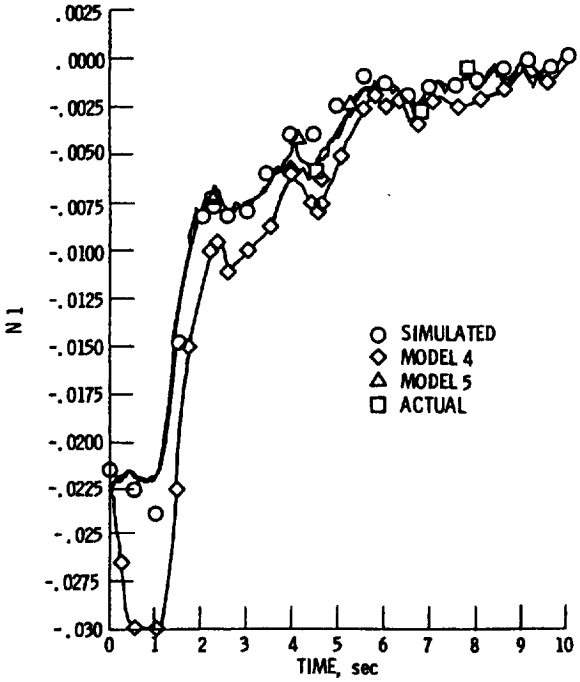

Figure 9.—A comparison of model predicted data with actual test data.

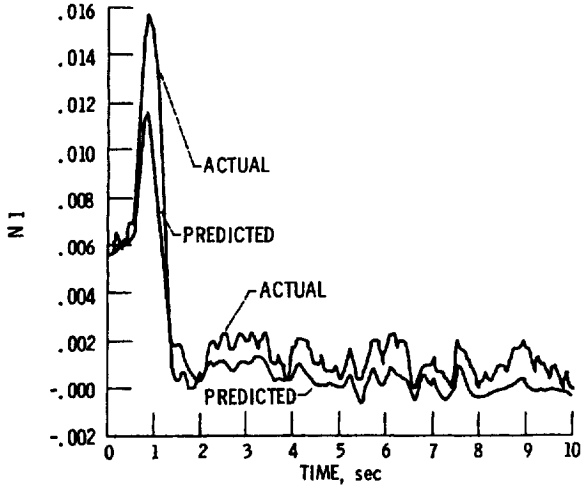

Figure 10.—Comparison of actual MVC output predicted by model 5 obtained from BOM data.

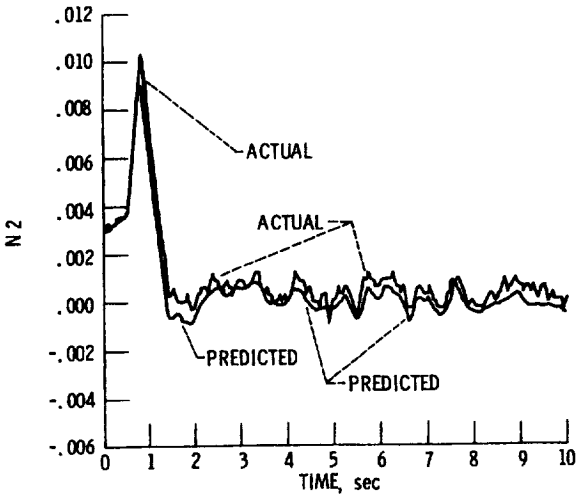

Figure 10.—Continued.

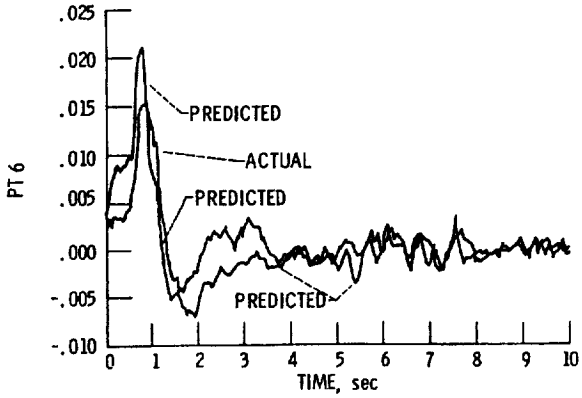

Figure 10.—Concluded.

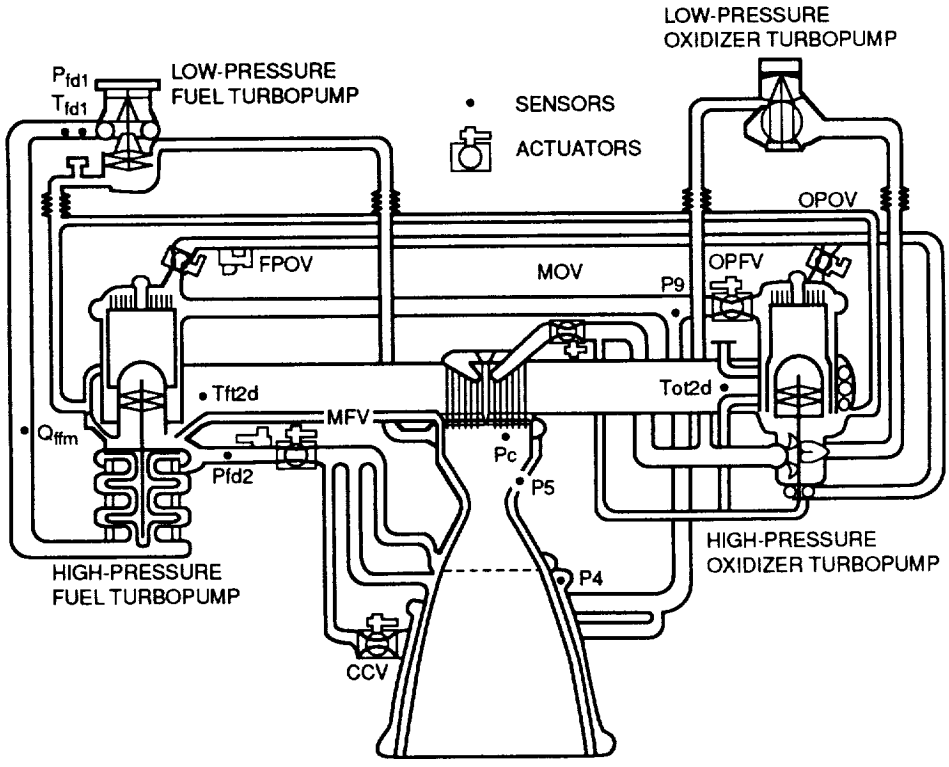

Figure 11.—Propellant flow schematic of the SSME.

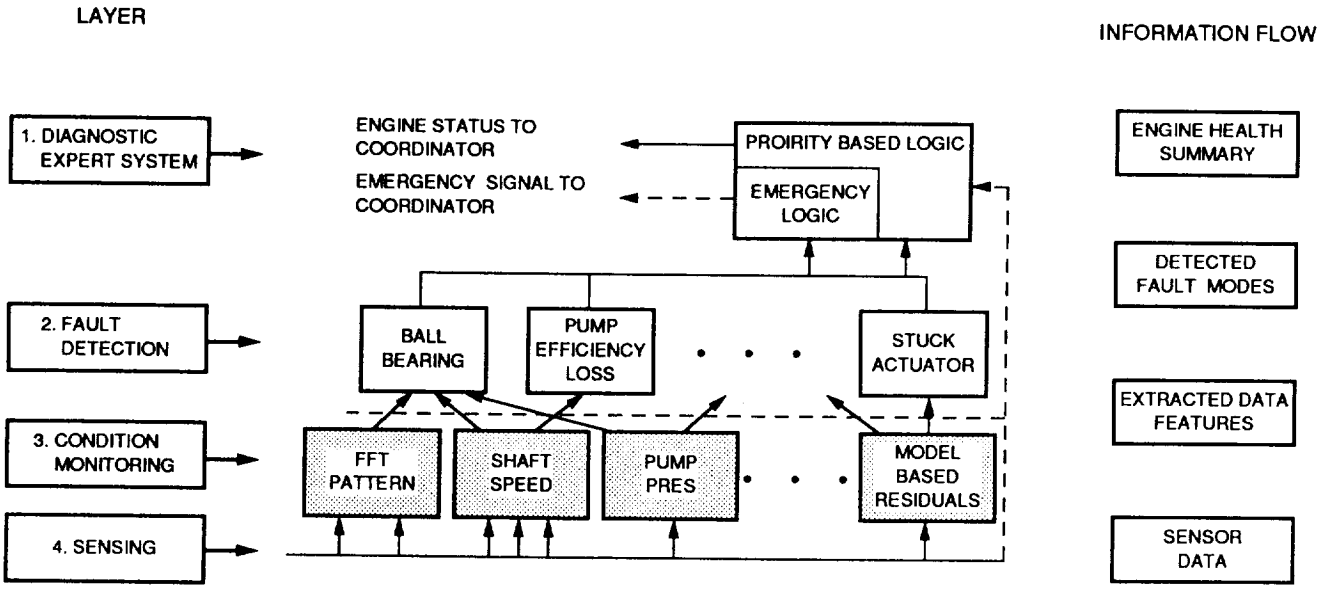

Figure 12.—Real-time diagnostic architecture.

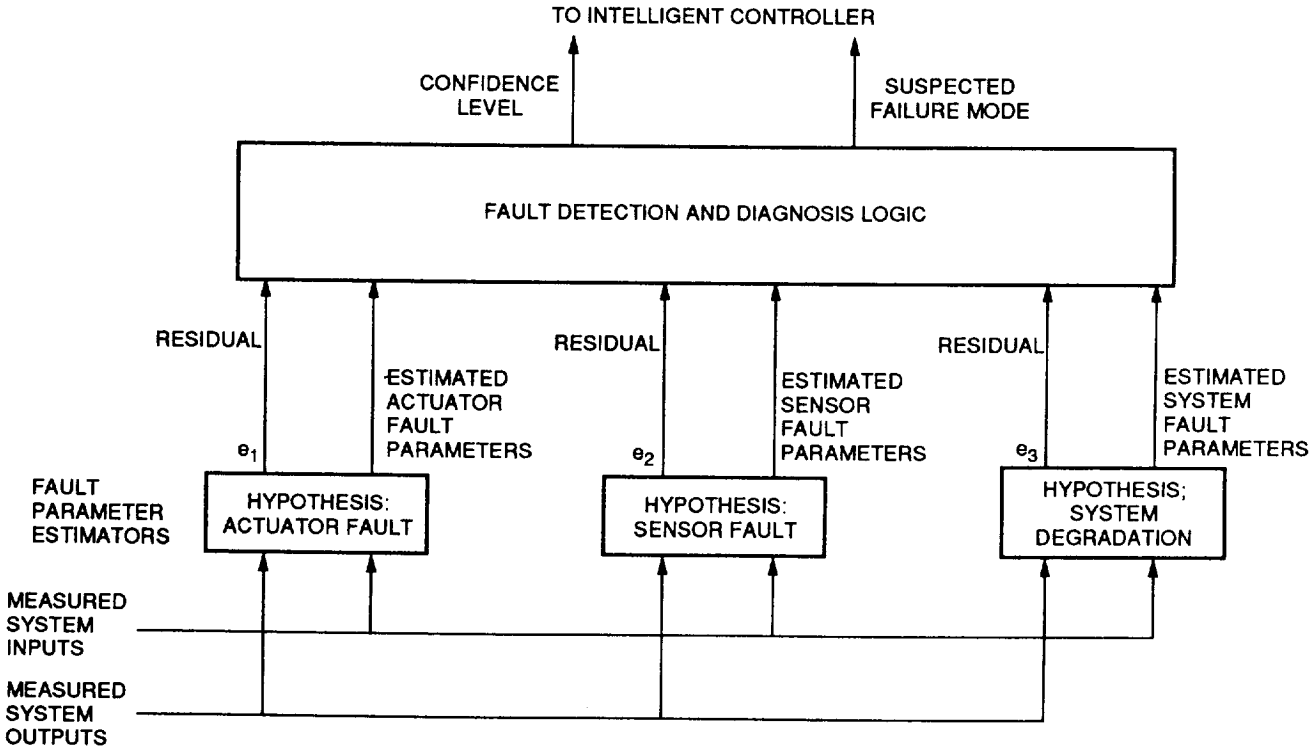

Figure 13.—Distributed fault diagnostic system.

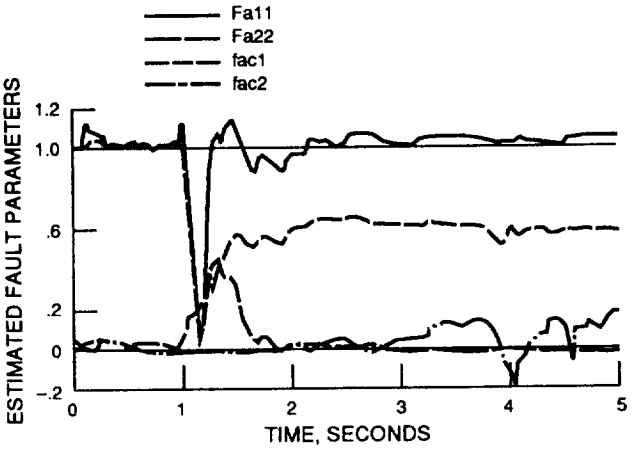

Figure 14.—Estimated fault parameters.

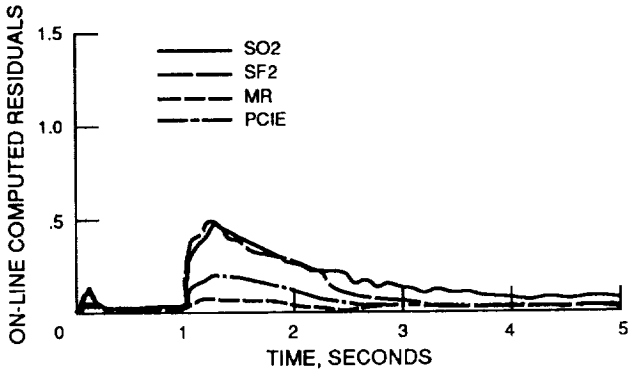

Figure 15.—Residual vector for actuator fault hypothesis.

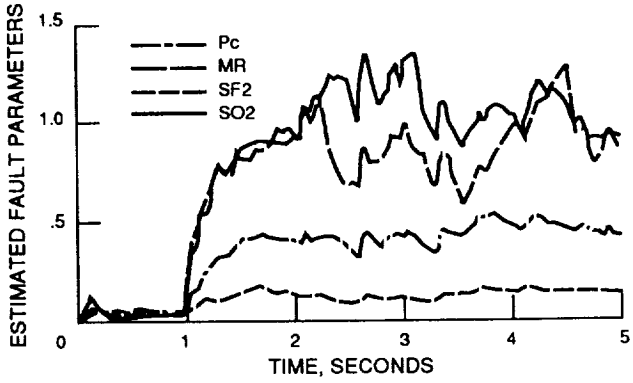

Figure 16.—Residual vector for system degradation hypothesis.

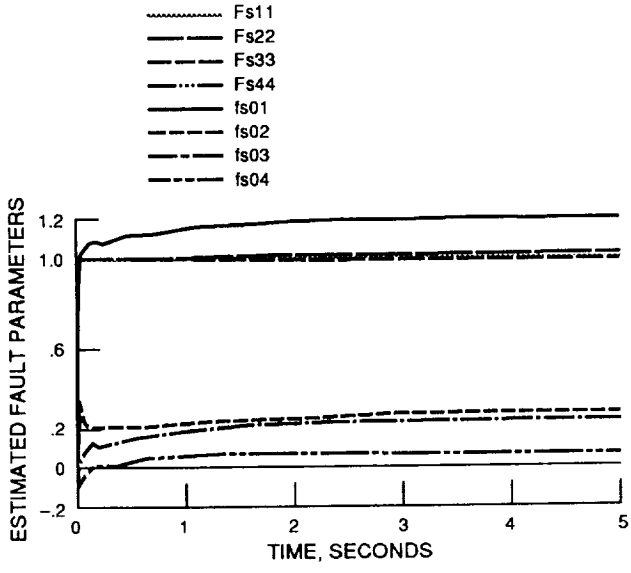

Figure 17.—Estimated fault parameters for PC bias fault.

REPORT DOCUMENTATION PAGE

Form Approved
OMB No. 0704-0188

1. AGENCY USE ONLY (*Leave blank*)	2. REPORT DATE	3. REPORT TYPE AND DATES COVERED
	August 1991	Technical Memorandum

4. TITLE AND SUBTITLE
Identification of Propulsion Systems

5. FUNDING NUMBERS
WU-506-42-72

6. AUTHOR(S)
Walter Merrill, Ten-Huei Guo, and Ahmet Duyar

7. PERFORMING ORGANIZATION NAME(S) AND ADDRESS(ES)
National Aeronautics and Space Administration
Lewis Research Center
Cleveland, Ohio 44135-3191

8. PERFORMING ORGANIZATION REPORT NUMBER
E-7171

9. SPONSORING/MONITORING AGENCY NAMES(S) AND ADDRESS(ES)
National Aeronautics and Space Administration
Washington, D.C. 20546-0001

10. SPONSORING/MONITORING AGENCY REPORT NUMBER
NASA TM- 106007

11. SUPPLEMENTARY NOTES
Prepared for a workshop sponsored by the Ohio Aerospace Institute, Cleveland, Ohio, August 9, 1991. Walter Merrill and Ten-Huei Guo, NASA Lewis Research Center, Cleveland, Ohio, and Ahmet Duyar, Florida Atlantic University, Boca Raton, Florida 33432, and Summer Faculty Fellow at NASA Lewis Research Center. Responsible person, Walter Merrill, (216) 433-6328.

12a. DISTRIBUTION/AVAILABILITY STATEMENT
Unclassified - Unlimited
Subject Category 07

12b. DISTRIBUTION CODE

13. ABSTRACT (*Maximum 200 words*)

This paper presents a tutorial on the use of model identification techniques for the identification of propulsion system models. These models are important for control design, simulation, parameter estimation, and fault detection. Propulsion system identification is defined in the context of the classical description of identification as a four step process that is unique because of special considerations of data and error sources. Propulsion system models are described along with the dependence of system operation on the environment. Propulsion system simulation approaches are discussed as well as approaches to propulsion system identification with examples for both air breathing and rocket systems.

14. SUBJECT TERMS
Identification; Fault detection; Propulsion; Closed loop; Canonical forms

15. NUMBER OF PAGES
32

16. PRICE CODE
A03

17. SECURITY CLASSIFICATION OF REPORT	18. SECURITY CLASSIFICATION OF THIS PAGE	19. SECURITY CLASSIFICATION OF ABSTRACT	20. LIMITATION OF ABSTRACT
Unclassified	Unclassified	Unclassified	